

Coherent cosmology: wave effects of FRBs and GWs.

Ue-Li Pen and collaborators

December 12, 2023

Gravitational Waves, Fast Radio Bursts

- ▶ Coherent, distant source of radiation
- ▶ Interference effects under multi-path propagation
- ▶ potential for diffraction limited measurements
- ▶ new regime: microlensing by stars (or DM)
- ▶ nanohertz GWs: breakdown of geometric lensing, effervescent images
- ▶ Kirchoff-Fresnel path integral
- ▶ Morse index, complex images: measure time delays in weak lensing

FRBs

- ▶ Coherent, distant source of radiation
- ▶ Scintillate under multi-path propagation
- ▶ sensitive to ns time delay propagating for gigaparsecs
- ▶ corresponds to strain $h \ll 10^{-26}$: far exceeds LIGO
- ▶ highly elongated antenna pattern: sensitive to longitudinal modes

FRB110523

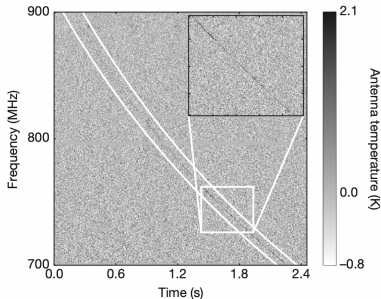
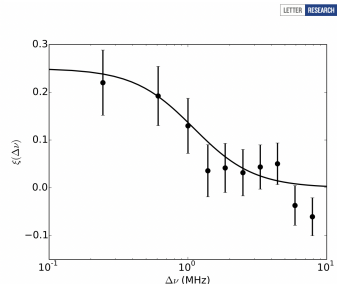


Figure 1 | Brightness temperature spectra versus time for FRB 110523. The diagonal black curve shows the pulse of radio brightness sweeping over time. The arrival time is differentially delayed (dispersed) by plasma along the line of sight. A pair of curves in white, bracketing the FRB pulse, show that the delay function matches the one expected from cold plasma. The grey horizontal bars show where data has been omitted owing to resonances within the GBT receiver. The inset shows fluctuations in brightness caused by scintillation.

Masui++ 2015, Nature, 528, 523



Extended Data Figure 1 | Spectral brightness correlation function of FRB 110523. The intensity spectrum has structure that is correlated for frequency separations less than $\Delta\nu_c = 1.2$ MHz. Error bars are the standard deviation of 3,208 simulated measurements with 817 independent noise realizations and are correlated.

precision astrometry

Picoarcsecond astrometry L39

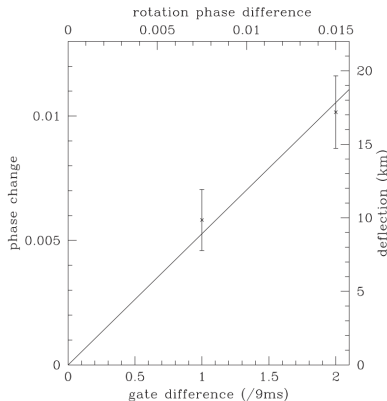


Figure 6. Pulsar motion projected along scattering axis. The horizontal axis is the time difference and the vertical axis is the apparent motion shift along the scattering axis, scaled to a Doppler frequency of -15MHz . The changes are always small. The error is about $1/1000\text{th}$ of a radian, which reflects the extremely high S/N of the measurement.

UP+14

Wave Microlensing

- ▶ spatially unresolved, echo of voltage stream delayed by microseconds
- ▶ search voltage stream, or look for scintillation
- ▶ observables: time delay, flux ratio
- ▶ sensitivity down to earth mass
- ▶ Jow+20

Microlensing: applications

- ▶ DM, stellar mass function, planets
- ▶ +plasma lensing: direct distance
- ▶ repeater macrolensing: direct distance
- ▶ contamination by plasma in lens galaxy?

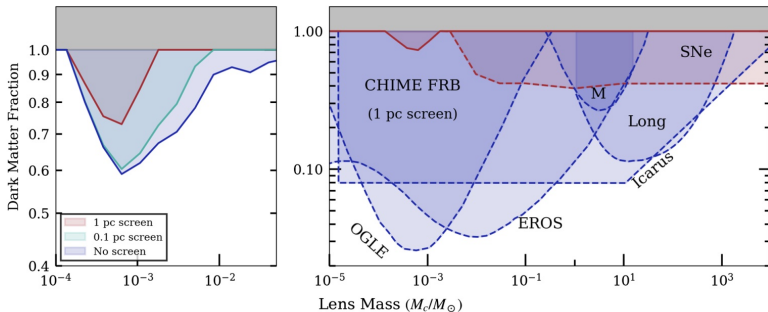


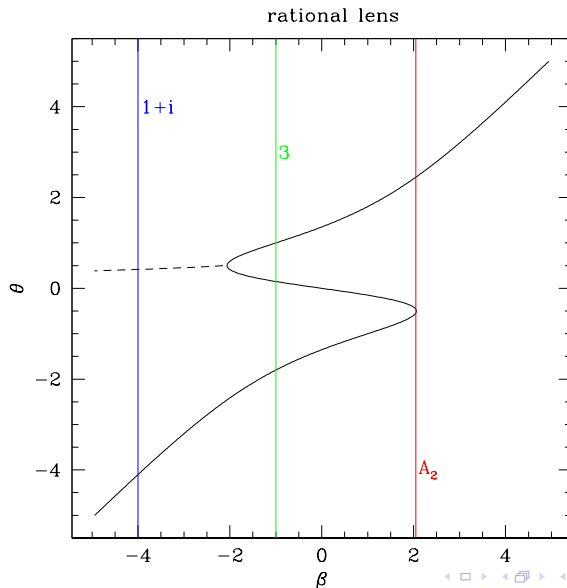
FIG. 5. Left: 95% constraints on PBHs as a function of scattering screen distance corresponding to the optical depth calculated in Fig. 3. We plot our fiducial (1 pc screen) model in red and suppress curves for screen distances of 10 and 100 pc because $\lambda < 3$ under those assumptions. Right: a collection of microlensing constraints on the fraction of dark matter composed of compact objects (such as PBHs), $f(M_c)$, assuming a monochromatic mass function peaked around M_c . We have shown Local Group PBH constraints in blue (M: MACHO [108], EROS [109], OGLE [30], Long: long-duration optical microlensing [110], Icarus [111]), and Local Universe constraints in red (SNe [11], CHIME/FRB, this work). CHIME/FRB lensing constraints depend on our two-screen scattering model, in which we have assumed that the average FRB is scattered by a screen at an effective distance of 1 pc, and our model for how DM correlates with distance. In these constraints, we have used Eq. (22) to define the exclusion limit as a function of M_c . Wave optics effects suppress our signal at $M \lesssim 1.5 \times 10^{-4} M_\odot$ and finite source size suppresses our signal at $M \gtrsim 3 \times 10^4 M_\odot$. This shows that coherent FRB lensing has the potential to search new parameter space for exotic compact objects such as PBHs.

Leung++22 (CHIME)

Effervescent Images

- ▶ consider “rational lens” potential $\psi(\theta) = \alpha/(1 + \theta^2)$
- ▶ Geometric/eikonal images at $\psi' = \theta$
- ▶ 5 roots. 1 or 3 real roots, rest imaginary
- ▶ P-L: at most one imaginary image contributes!
- ▶ imaginary image can be brighter than unlensed real image

Rational 1-D lens



New Observables

- ▶ for coherent sources: FRBs, pulsars
- ▶ weak lensing: imaginary image allows time delay measurement (Jow+21)
- ▶ strong lensing: delay measurements enable measurement of co-linearity (Jow++21)
- ▶ microlensing: instant time delay, planets (Jow+20)
- ▶ macrolensing: potentially nano-second delay – universe expands! Dark energy, etc (Wucknitz+21)
- ▶ dimensionless strain cm/Gigalightyears $h \sim \Delta t/t \sim 10^{-26}$: competitive with LIGO, etc

Macro lensing

A&A 645, A44 (2021)

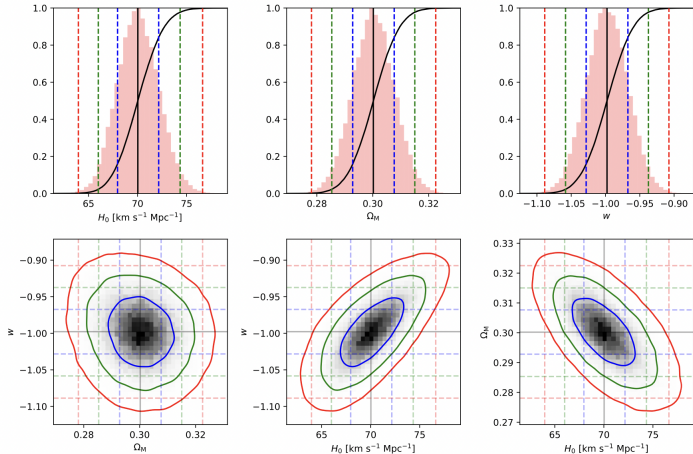
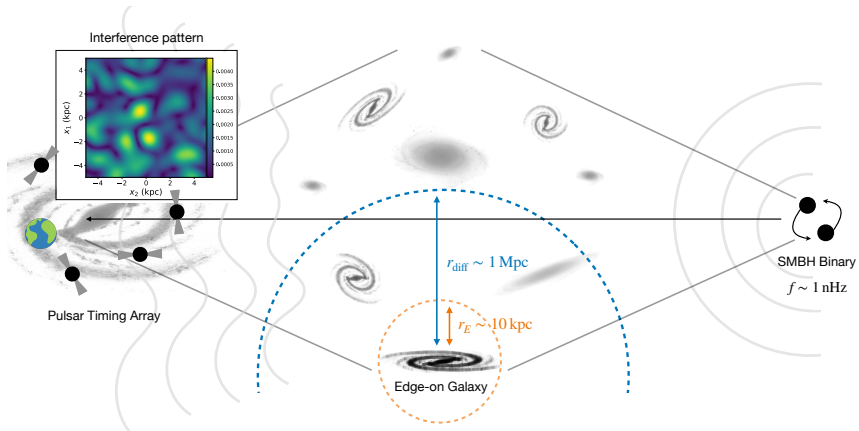


Fig. 3. Posterior distribution of H_0 , Ω_M and w using all lenses simultaneously. The *upper row* shows marginalised distributions for individual parameters, the *lower row* for all combinations of two. See Fig. 2 for a detailed description.

Wucknitz, Spitler, ULP 2021, A&A, 645, A44

Diffraction Gravitational Wave Lensing



Jow+ in prep

Discussion

- ▶ Eikonal effects applicable to coherent sources, e.g. FRBs, pulsars, LIGO/Lisa GWs
- ▶ microlensing down to planet size
- ▶ full wave effect dominates for long wavelengths as Fresnel scale is bigger than Einstein radius, i.e. PTA GWs

Conclusions

- ▶ wave optics changes nature of astrophysical observables: Coherent FRB/pulsar/GW radiation one of the potentially most precise measurements in physics
- ▶ already makes pico-arcsecond images of pulsars
- ▶ ISM plasma screens modelled quantitatively as localized 1-D features, no longer stochastic turbulent volume.
- ▶ Picard-Lefschetz theory provides alternative interpretation of optics, quantum mechanics: imaginary positions and trajectories
- ▶ next generation FRB telescopes for cosmic mass inventory, possibly dark energy/acceleration
- ▶ PTA weak diffractive lensing may give new tool for Hubble Constant tension